AeroChem TP-333 NASA CR-144928

NO_x DEPOSITED IN THE STRATOSPHERE BY THE SPACE SHUTTLE SOLID ROCKET MOTORS

Harold S. Pergament
Roger D. Thorpe
Baochuan Hwang

Final Summary Report

Phase II

December 1975

Prepared under Contract No. NAS1-13544 by
AEROCHEM RESEARCH LABORATORIES, INC.
Princeton, NJ

for

NATIONAL AERONAUTICS AND SPACE ADMINISTRATION

Page intentionally left blank

ABSTRACT

This report extends the work completed under Phase I of this contract which presented the initial predictions of NO_x deposited in the stratosphere (at 30 km) by the space shuttle SRM's. The earlier work assumed that the two SRM's could be replaced by an "equivalent" single nozzle and, as such, neglected such effects as the intersection of the two SRM plumes and mixing of the rocket exhaust products and ambient air in the base recirculation region. The present work demonstrates that these phenomena will not influence the total NO_x deposition rate. In addition it is shown that uncertainties in Al_2O_3 particle sizes, size distributions and particle/gas drag and heat transfer coefficients will not have a significant effect on the predicted NO_x deposition rate.

The final results of this study show that the total mass flow of NO_x leaving the plume at 30 km altitude is 4000 g/sec with a possible error factor of of $\frac{\times}{\div}$ 3. For a vehicle velocity of 1140 meter/sec this yields an NO_x deposition rate of about 3.5 g/meter. The corresponding HCl deposition rate at this altitude is about a factor of 500 greater than this value.

Page intentionally left blank

TABLE OF CONTENTS

LIST OF TABLES

LIST OF FIGURES

LIST OF FIGURES (continued)

I. INTRODUCTION

This study was directed towards determining the total amount of NO_x that the Space Shuttle Solid Rocket Motors (SRM) will deposit while passing through the stratosphere. The results (together with the corresponding HCl deposition rate) will be used as input to stratospheric diffusion/chemistry models (e.g., Ref. 1) to determine the effects of the SRM exhausts on stratospheric ozone concentrations. The approach taken here has been to use state of the art gasdynamic/chemistry models, that include the effects of nonequilibrium gas/particle flow on gas properties and composition, for predicting NO_x concentrations within the SRM nozzle and plume. Although NO_x concentrations at the nozzle exit plane, incorporating the above effects, can be calculated with existing computer codes, the complex interactions arising from the intersection of the plumes from the two SRM's and three space shuttle main engines cannot readily be treated with existing models. Figure 1, a schematic (to approximate scale) of the booster/orbiter plumes at 30 km altitude, indicates the difficulty in modeling the near field. The flow is asymmetrical; the plumes from the liquid H_2/O_2 engines intersect the SRM plumes at the top and there is a significantly large base recirculation region at the bottom. In addition, the SRM plumes intersect within a short distance from the exit, resulting in a large interaction region.* Figure 2 shows the plume far field, the total length of about 2500 ft being the length of the "NO_x plume" computed in Ref. 2. From this schematic it appears reasonable to assume that, for the purpose of computing the total NO_x deposition rate, the plume emanates from an "equivalent" single nozzle having the same total mass flow as the two SRM's. Thus in the present study we calculated the total NO_x deposition rate at 30 km using an equivalent single nozzle approach and then determined whether the intersection of the SRM plumes and combustion of SRM exhaust products in the shuttle base recirculation region could increase this calculated value.

There are three high temperature regions where NO_x is likely to be produced: the combustion chamber, the mixing/afterburning regions of the plume and downstream of strong shocks in the plume. The schematic shown in Fig. 3 indicates the single plume afterburning region in the near field and the strongest shock in the plume, the first Mach disc. (Also shown is the Al_2O_3 particle cloud which remains close to the core of the plume.) The NO_x mass fraction at the nozzle exit plane is smaller than that in the chamber due to recombination during the expansion process. Any increase in NO_x mass

---

* The total length of the shuttle booster is about 186 ft; the strong plume interaction region occurs within about 300 ft of the SRM nozzle exit plane.

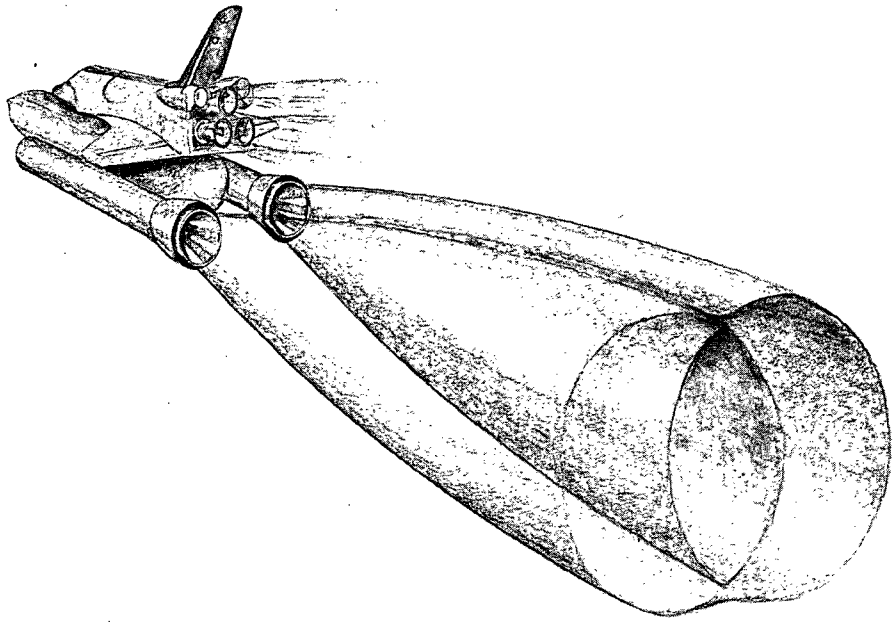

FIG. 1 NEAR FIELD SCHEMATIC OF SPACE SHUTTLE EXHAUST PLUMES IN THE STRATOSPHERE

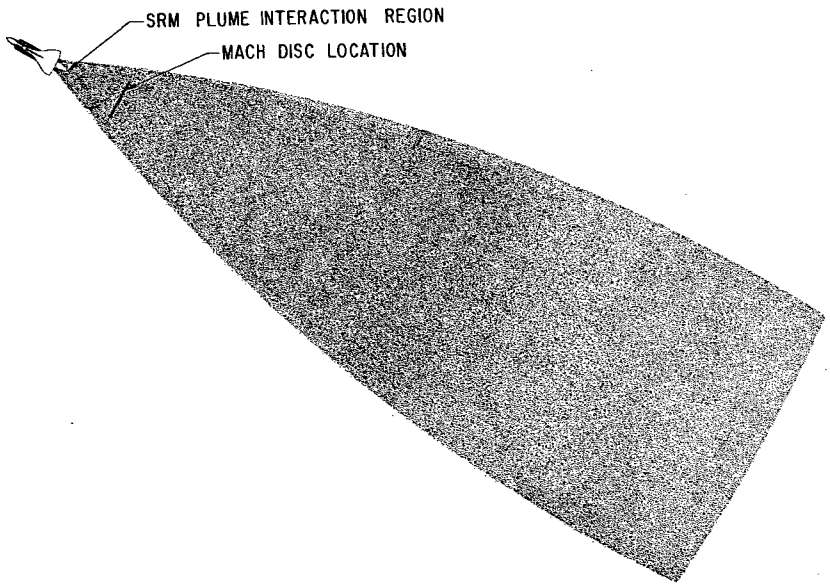

FIG. 2 FAR FIELD SCHEMATIC OF SPACE SHUTTLE EXHAUST PLUMES IN THE STRATOSPHERE

Scale: 1" ≈ 250 ft; Total "NO_x" plume length ≈ 2500 ft

fraction in the plume is described via the local plume enhancement factor (LPEF) shown schematically in Fig. 4. The influence, if any, of afterburning and shocks is to increase the LPEF until it reaches an asymptotic value, the overall plume enhancement factor (OPEF), which defines the end of the "NO_x plume". Therefore, multiplying the mass flow of NO_x leaving the nozzle by the OPEF gives the mass flow of NO_x "leaving" the plume.

Reference 2 summarizes the equivalent single nozzle calculations* and gives the first determination of the total amount of NO_x deposited in the stratosphere by the SRM's. The results show that the NO_x mass flow "leaving" the plume (at 30 km) is 4000 g/sec with a possible error factor of 4. For a velocity of 1140 m/sec the NO_x deposition rate is then about 3.5 g/meter. This value can be used as "line source" input data to a two-dimensional stratospheric diffusion model, assuming the deposition rate is constant throughout the stratosphere.

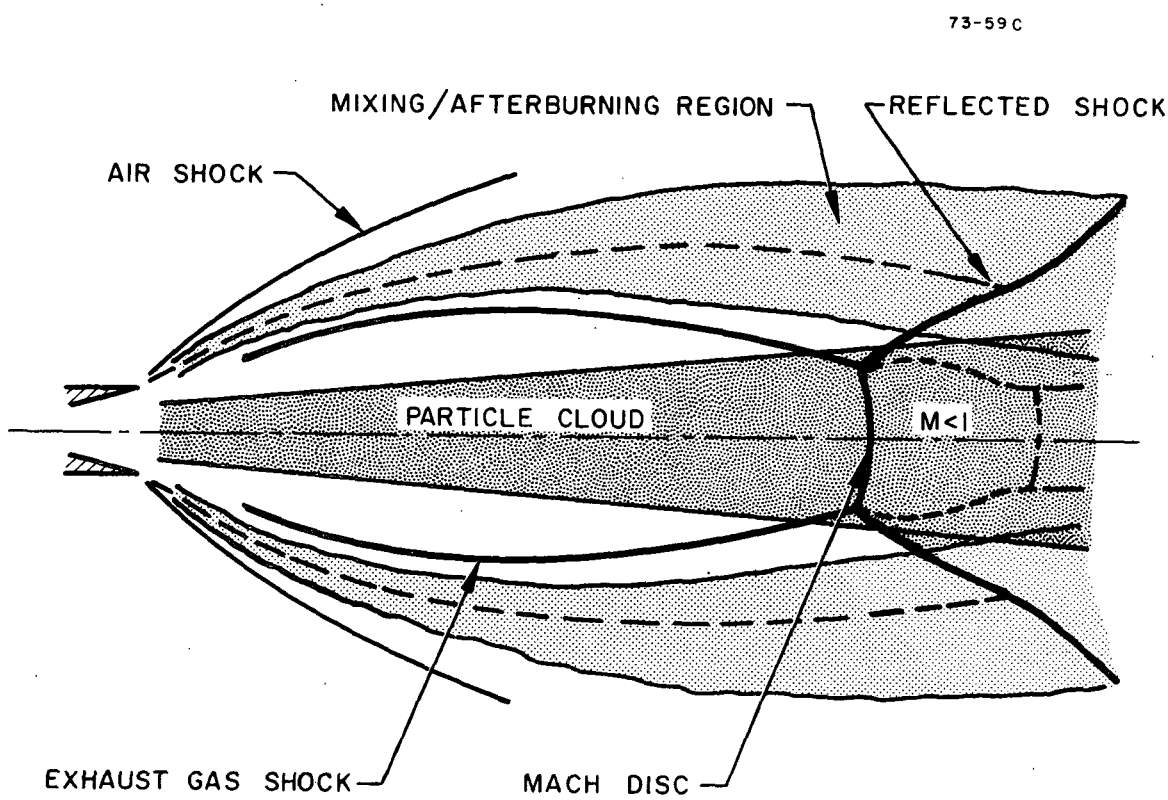

FIG. 3 SCHEMATIC OF NEAR FIELD OF EQUIVALENT SINGLE NOZZLE PLUME

* This is the report on Phase I of this contract and should be read before reading the present report.

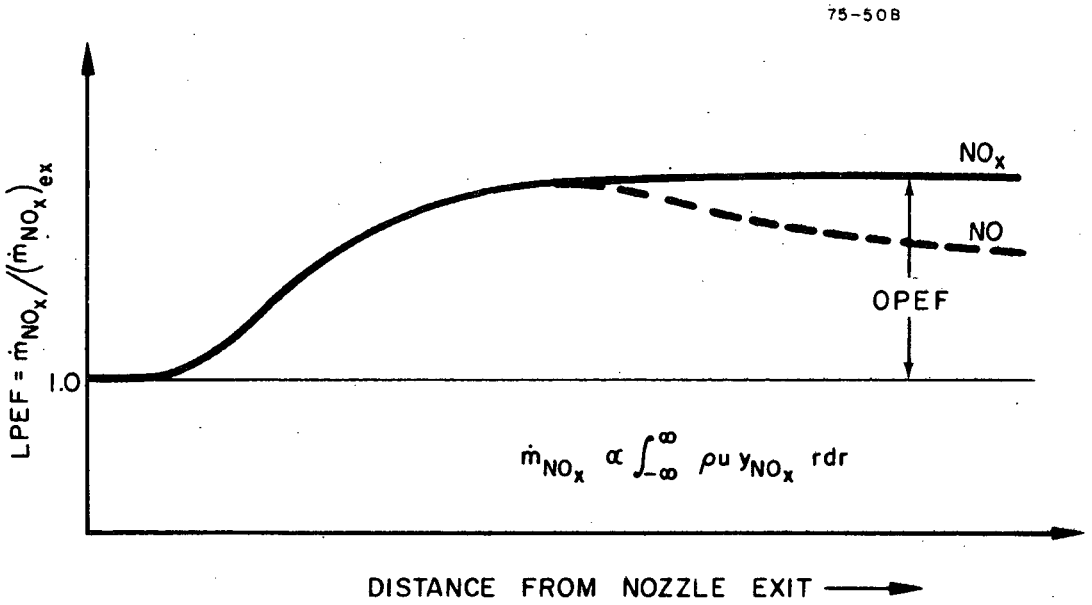

FIG. 4 SCHEMATIC SHOWING DEFINITIONS OF LOCAL PLUME ENHANCEMENT FACTOR (LPEF) AND OVERALL PLUME ENHANCEMENT FACTOR (OPEF)

In Phase II of this contract (the subject of this report) we have studied the following three separate effects that could potentially increase the NO_x deposition rate over that predicted from the equivalent single nozzle analysis:[2] (1) uncertainties in the Al_2O_3 particle sizes, size distributions and particle/gas drag and heat transfer coefficients used in the SRM nozzle calculations, (2) intersection of the two SRM plumes and (3) combustion of SRM exhaust products in the shuttle base recirculation region.

II. SRM NOZZLE FLOW

A. Analysis

The Al_2O_3 particles produced in the combustion chamber, will, in general have different temperatures and velocities than the gas during their passage through the nozzle and into the plume (see, e.g. Ref. 3). Nozzle codes which do not account for this gas/particle nonequilibrium effect can give inaccurate results.[3] However, the results obtained from a nozzle code that correctly accounts for gas/particle nonequilibrium effects must be critically evaluated in terms of the accuracy of the particle parameter input data, particularly mean particle size, size distributions and drag/heat transfer coefficients. The quantitative influence of uncertainties in Al_2O_3 particle parameters on nozzle exit plane properties is demonstrated in this section.

For the present study the AeroChem-developed FULLNOZ code[4] was used to calculate gas and particle properties within the SRM nozzle. FULLNOZ

treats coupled gas/particle nonequilibrium flows in two-dimensional (axisymmetric) nozzles, including the effect of the wall boundary layer on gas properties along the "inviscid wall" streamline.* The results of our initial calculations of nozzle exit plane properties were reported in Ref. 2. (Table I gives the SRM propellant composition and chamber properties.) Figure 5 shows the

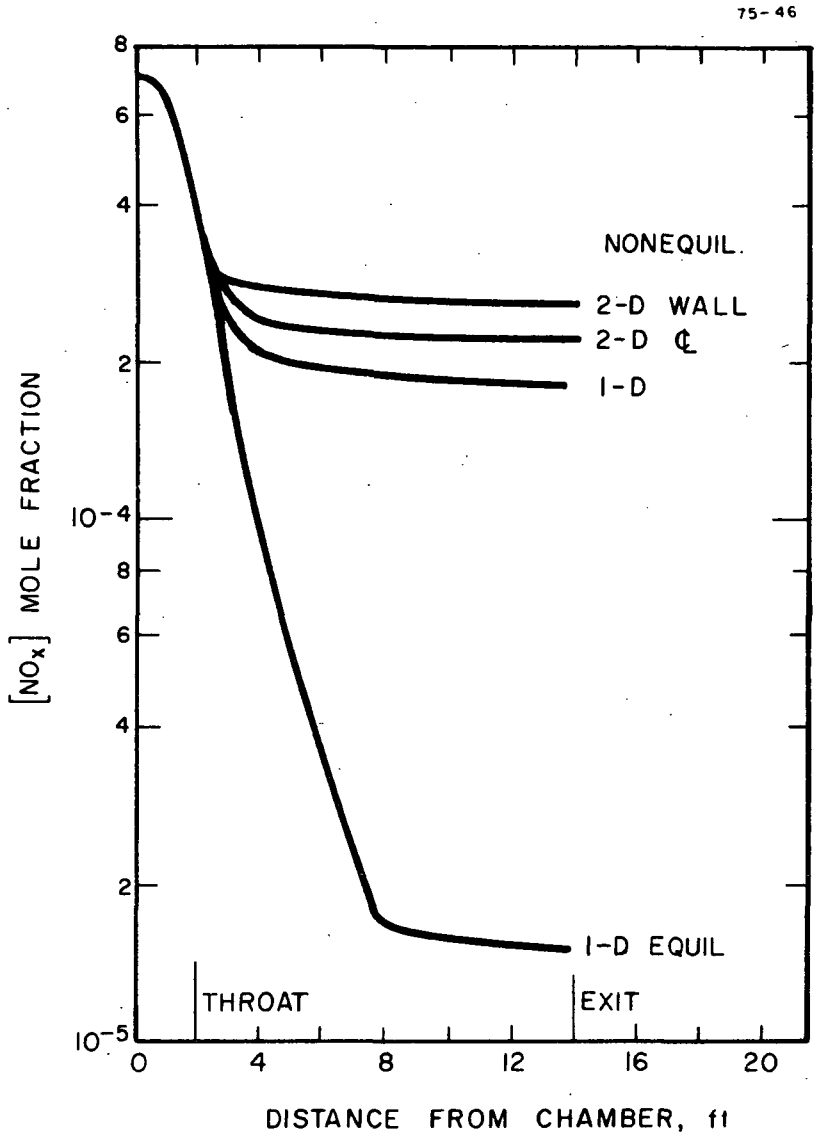

FIG. 5 NO_x MOLE FRACTION IN SPACE SHUTTLE SRM NOZZLE
A comparison between 1-D equilibrium, 1-D kinetic and 2-D kinetic calculations

---

* FULLNOZ is designed for high Reynolds number flows in which boundary layer effects do not propagate far from the wall.

TABLE 1. SPACE SHUTTLE SRM PROPELLANT COMPOSITION AND CHAMBER PROPERTIES

Propellant Composition	Wt. %	ΔH_f^o (kcal/mole)
NH_4ClO_4	69.6	-70.69
Al	16.0	0.0
$C_{6.884}H_{10.089}O_{0.218}N_{0.264}$	12.0	-12.0
$C_{6.15}H_{6.97}O_{1.17}N_{0.03}$	2.0	-28.3
Fe_2O_3	0.4	-197.3

	Chamber[a]
Pressure, atm	41.6
Temperature, °K	3400
Mass fraction Al_2O_3 particles	0.30

Gas Composition, Mole Fraction

CO	2.49(-1)
CO_2	1.74(-2)
HCl	1.43(-1)
H	3.80(-2)
H_2	2.77(-1)
OH	9.11(-3)
H_2O	1.52(-1)
N_2	9.92(-2)
N	6.19(-6)
NO	7.05(-4)
O	7.45(-4)
O_2	1.62(-4)
Cl	1.30(-2)
HNO	1.15(-6)
N_2O	7.93(-8)
NH	2.78(-6)
NH_2	1.07(-5)

[a] Thermochemical equilibrium calculations; nozzle area ratio, $A/A^* = 6.7$ and nozzle exit radius = 185 cm.

NO_x mole fraction distribution within the nozzle for one-dimensional (1-D) and two-dimensional (2-D) kinetic calculations. The 2-D calculations were made using, as input data, particle sizes and size distributions obtained from the experimental work of Smith et al[5] and Miller and McCarty.[6] The possibility of errors in applying these correlations to the SRM nozzle flow was one motivation for the present parametric study.

Another factor influencing the determination of nozzle and plume gas properties is the proper value to use for the gas/particle drag and heat transfer coefficients which enter directly into the gas/particle coupling terms in the momentum and energy equations.[4] The most widely accepted drag coefficients are those developed by Crowe[7] who correlated data on small diameter spheres from continuum to free molecular flows and also gave expressions for heat transfer coefficients. However, these correlations are also subject to uncertainty and parametric variations of the drag and heat transfer coefficients are needed to properly assess their effects on nozzle and plume gas properties. Thus to determine the sensitivity of the calculated results to the above-mentioned uncertainties in input parameters, the mean particle sizes, size distributions, heat transfer and drag coefficients were varied over a wide range (these are summarized in Table II). Nozzle wall temperature is also included as a parameter because it influences the shear stress and heat transfer within the boundary layer which, in turn, influences the gas velocity and temperature along the inviscid wall streamline.

In order to substantially reduce computer run times the parametric calculations were made assuming frozen gas-phase chemistry.* Utilizing a chemical reaction mechanism of the type reported in Ref. 2 will result in increased absolute values of the nozzle exit plane temperatures (e.g. for the SRM frozen exit plane temperatures of $\approx$ 2000 K would increase to $\approx$ 2200 K by including nonequilibrium chemistry in the nozzle calculations) with approximately the same pressure distribution. The incorporation of nonequilibrium chemistry will not, however, change the relative effects on nozzle and plume gas properties of varying particle sizes and drag coefficients. This study concentrates particularly on the nozzle exit plane properties. If the results show that varying the input parameters gives little difference in predicted exit plane properties we can state with certainty that there will be a negligible influence on plume properties and therefore, a negligible influence on the NO_x deposition rate.

---

* Radical recombination on the surface of the Al_2O_3 particles was also neglected in this study.

TABLE II. PARAMETRIC VARIATIONS IN PARTICLE PROPERTIES

Case No.	Particle Sizes radius (μ)/wt.%	Drag/Heat Transfer Coefficients	Wall Temperature, °K
STD	4/50 6/30 8/15 10/5	STD	1500
1	4/100	STD	1500
2	8/100	STD	1500
3	4/10 6/40 8/40 10/10	STD	1500
4	STD radii × 2	STD	
5	STD	STD	3000
6	STD	STD	800
7	STD	STD × 5	1500
8	STD	STD × 0.2	1500
9	STD	STD	No Boundary Layer

B. Results

The most important exit plane gas properties (i.e., those which influence the plume shock positions and "degree of afterburning") are pressure, temperature and Mach number. The nozzle exit plane pressure distributions given in Fig. 6 are typical for bell-shaped nozzles, where pressures at the axis are less than those at the nozzle lip (in this case by about a factor of 2). Only cases 4, 7 and 8 differ from the standard case. Doubling the particle radius drops the pressure by less than 10% (on the average) while varying the drag/heat transfer coefficients by a factor of 5 (which is probably well beyond the range of uncertainty for these coefficients) from their standard values is seen to result in a slightly larger deviation from the standard case. The other cases result in practically no deviation from the standard case. The effects of these parametric variations on gas temperature and Mach number distributions, shown in Figs. 7 and 8, are essentially the same. The temperature distributions generally follow the pressure distributions up to $R/R_{ex} \approx 0.8$,* where the limiting particle streamlines are reached (see Fig. 9),

* R is radial distance from the centerline; R_{ex} is nozzle exit radius.

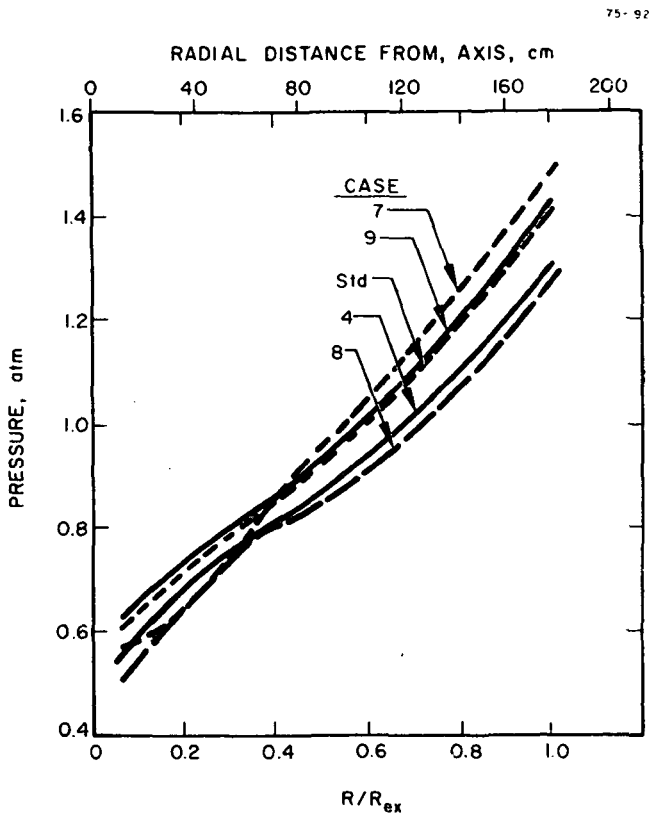

FIG. 6 SRM NOZZLE EXIT PLANE PRESSURE DISTRIBUTIONS
Cases explained in Table II

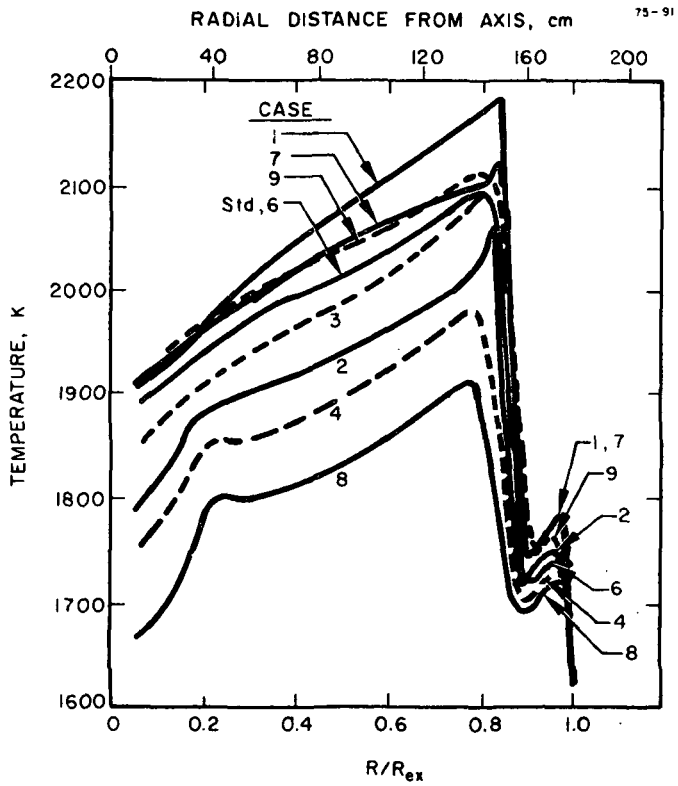

FIG. 7 SRM NOZZLE EXIT PLANE GAS TEMPERATURE DISTRIBUTIONS
Cases explained in Table II

FIG. 8 SRM NOZZLE EXIT PLANE MACH NUMBER DISTRIBUTIONS
Cases defined in Table II

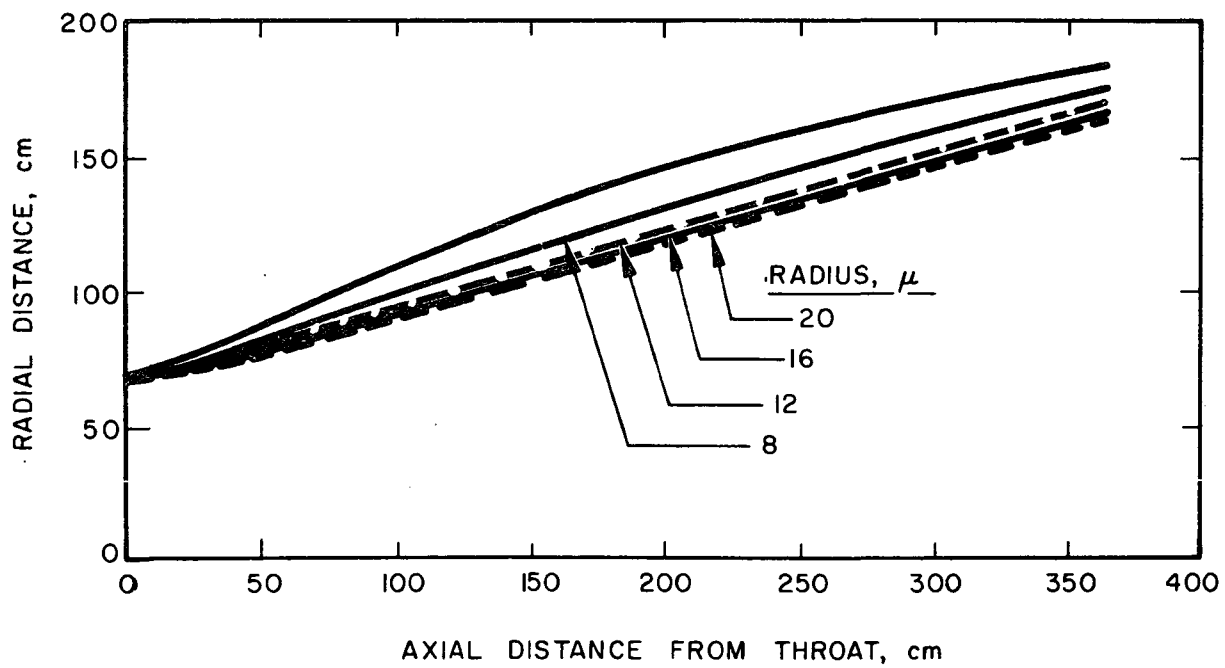

FIG. 9 SRM NOZZLE CONTOUR AND LIMITING PARTICLE STREAMLINES

after which the temperatures drop sharply, go through a "hump" and finally reach the inviscid wall temperature (not the actual wall temperature used in the boundary layer calculations). A comparison between the standard case and cases 1 to 4 shows that the biggest effect occurs when the mean particle sizes are doubled. However this only results in average temperature changes of ≈ 100 K, which are negligible. The largest effect in the parametric study occurred when the drag/heat transfer coefficients given by Crowe[7] were reduced by a factor of 5, and this only reduces the temperature by about 200 K on the average. This temperature change will not have a major effect on NO_x concentrations leaving the nozzle or on the enhancement of NO_x concentrations by the plume. Figure 10 shows a typical plot of exit plane gas and particle tempera-

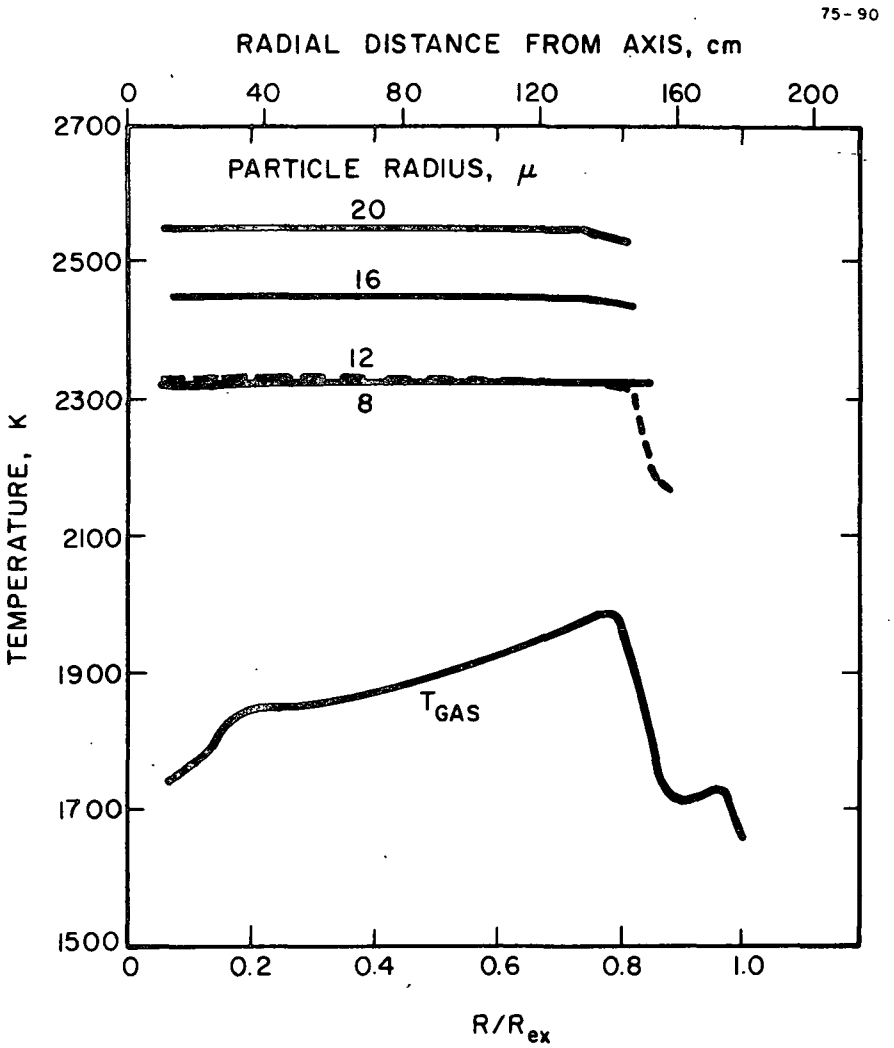

FIG. 10 NOZZLE EXIT PLANE GAS AND PARTICLE TEMPERATURE DISTRIBUTIONS FOR CASE 4
(See Table II)

tures for case 4. Particle temperatures are seen to be nearly constant across the exit plane, with the smallest particles at their solidification temperatures.

An independent study of the influence of particle parameters on exit plane properties was carried out by Lockheed/Huntsville using a similar type of nozzle code.[8] Some preliminary results were presented to NASA/Langley by B. Roberts[9] of NASA/JSC. Their results (which are consistent with those reported herein) showed that only negligible (or minor) differences in predicted values of the initial plume inclination angle (which depends on the gas properties at the nozzle lip) occurred due to uncertainties in particle sizes, distributions and drag and heat transfer coefficients.

Based on this parametric study we conclude that uncertainties in particle sizes, size distribution and gas/particle drag and heat transfer coefficients will not have a significant influence on predictions of the total amount of NO_x deposited in the stratosphere by the space shuttle SRM's.

III. INTERSECTING SRM PLUMES

A. Model of the Plume Interaction Region

Figure 11 shows the interaction between plumes from the two SRM boosters* (to approximate scale; R_{ex} = 185 cm) and the reflection of the exhaust gas shocks. The impingement of the base region recirculated flow should be accounted for in analyzing the interaction region since it may prevent the two exhaust gas shocks from intersecting at a point (as shown in Fig. 11). The schematic structure of the interaction region, including base flow recirculation, is shown in Fig. 12. The separation distance, AB, is proportional to the base pressure in the region between the two nozzles. The exact base pressure is of course not known, but it can be expected to be only slightly different from the ambient pressure† at the altitude of interest because the mixing flow in the base region is vented out through a very large gap area between the two nozzles (see e.g. Refs. 11, 12). Consequently it is reasonable to assume that the exhaust gases in the mixing zone of the jet boundaries cannot penetrate downstream into the high pressure area behind the intersection of the two jets and that the two shocks will, in fact, intersect at a point, as indicated in Fig. 11.

---

* In this analysis the potential effects of the exhaust plumes from the H_2/O_2 orbiter motors have been assumed to be negligible.

† In a private communication, Chul Park of NASA/AMC[10] said that measurements on a scale-model shuttle vehicle at 30 km (Mach number = 3.75) in the Ames 11 foot supersonic tunnel showed the base pressure to be approximately equal to the ambient pressure.

FIG. 11 MODEL OF THE SRM PLUME INTERACTION REGION

FIG. 12 SRM PLUME INTERACTION REGION, INCLUDING BASE FLOW RECIRCULATION

The reflected shock shape was calculated by: (1) using pre-shock properties obtained from the AeroChem Atmospheric Plume Interaction Program (AIPP Code[13,14]) with the exact initial flow properties at the nozzle exit (calculated from FULLNOZ[4]) as input and (2) assuming that the post-shock flow direction was parallel to the centerline of the two nozzles. The results of these calculations show that the reflected shock wave angle decreases only about one degree per downstream distance equal to the nozzle exit radius. Hence, the curved reflected shock was modeled by two straight sections: the first having the same angle as the initial reflected shock (14.6 deg) at the point where the two exhaust gas shocks intersect, while the second is parallel to the axis starting at the point where the actual shock becomes parallel to the axis. This (conservative) model was selected because it allows the maximum possible mass flow through the shock.

B. Estimation of Total Amount of NO_x Flux in Interaction Region

In order to determine an approximate trend for NO_x production in the interaction region, the species composition was calculated assuming chemical equilibrium at several temperatures higher than (for conservatism) or equal to the temperature behind the reflected shocks. These calculations showed that the mass fraction of NO_x at the highest temperature (3000 K) increased by about a factor of 8. However, chemical kinetic calculations in the interaction region are required to give more realistic results. These calculations were made along a streamline with a specified pressure distribution and initial conditions given by the calculated post-shock properties at the point of intersection of the two shocks (temperature = 2335 K). The chemical reaction mechanism was identical to that used for the initial plume [NO_x] prediction given in Ref. 2. The results, shown in Fig. 13, indicate almost no change in the mass fraction of NO_x. In order to obtain an upper estimate of NO_x production in this region another kinetic calculation was made using a very high initial temperature, 3000 K.* This result also showed a negligible increase in NO_x mass fraction. Thus the predicted equilibrium increase in NO_x mass fraction cannot practically be realized.

From the above analysis we conclude that the oblique shocks resulting from the intersection of the two SRM plumes do not act as a direct source of NO_x in the plume.

---

* The temperature behind the Mach disc is $\approx$ 3400 K.[2]

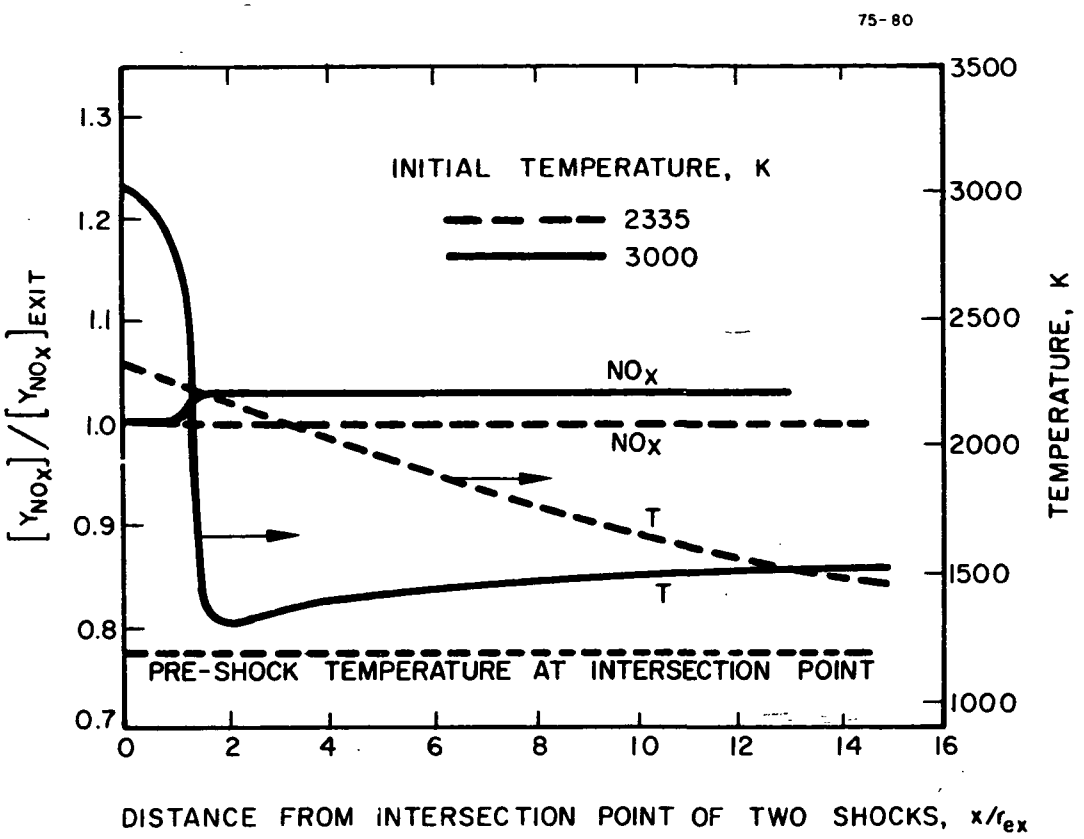

FIG. 13 NO_x MASS FRACTION RATIO AND TEMPERATURE DISTRIBUTIONS IN INTERACTION REGION, KINETIC CALCULATIONS

$(Y_{NO_x})_{exit}$ = NO_x mass fraction at nozzle exit plane

IV. POTENTIAL EFFECTS OF SHUTTLE BASE REGION COMBUSTION

Because the design of the space shuttle provides a large base region between the two SRM's, a significant flow recirculation area exists in which mixing and combustion (rocket exhaust products/ambient air) can occur (see Fig. 14). If ignition takes place in the base region the high temperature combustion products can be entrained at the cooler air/plume interface and the increased quantities of free radicals in the plume (H, OH, etc.) would initiate or speed up the chain-branching H_2/O_2 combustion reactions (afterburning).*

* The base would then, in effect, act as a flameholder. This "flameholding" effect was observed[15] in flights of the Apollo first stage, which uses five F-1 (LOX/kerosene) engines.

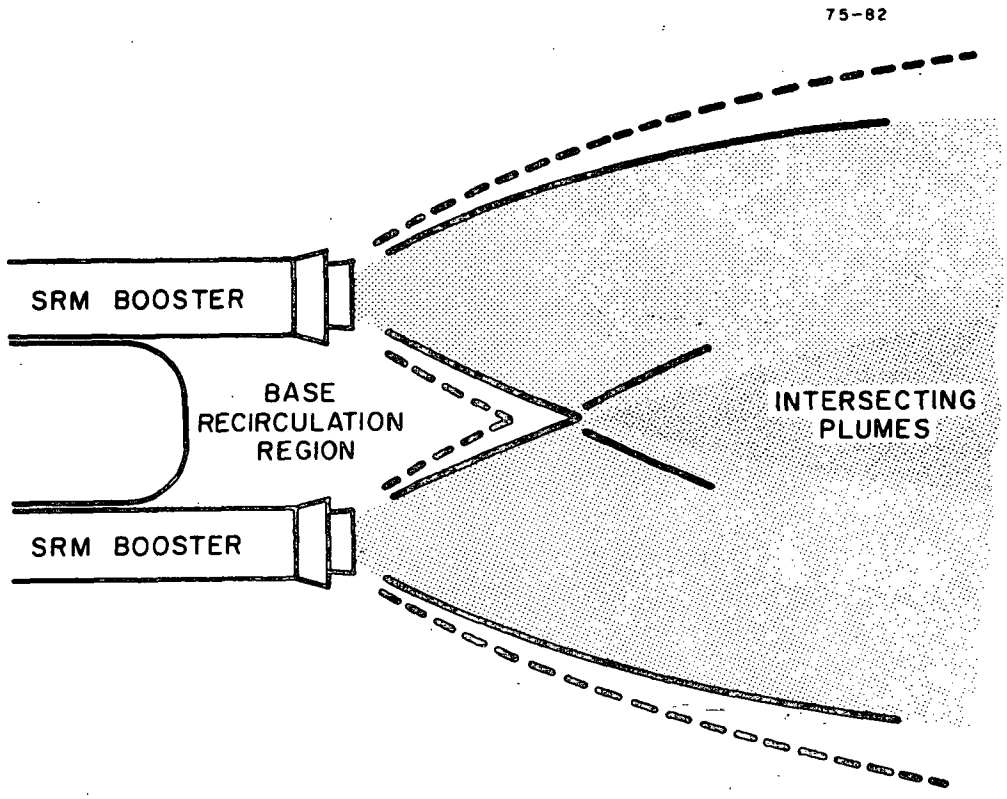

FIG. 14 SCHEMATIC OF SPACE SHUTTLE BOOSTER BASE RECIRCULATION REGION

This is a potentially important consideration in determining the total NO_x deposition rate in the stratosphere since it has already been shown[2] that, with no source of high temperature combustion products entrained in the plume, the influence of afterburning (at 30 km) on $[NO_x]$ production is negligibly small. The goal of this work, therefore, was to quantitatively determine the influence (on the NO_x deposition rate) of a small amount of combustion products entering the plume in the base region.*

A. Analysis

The approach taken was to use the base region combustion products as an (axisymmetric) annular boundary condition to an equivalent single nozzle plume calculation. In fact, any base region combustion products would enter the plume between the two SRM's rather than on the outside. The above assumption was made in order to conveniently use a parallel mixing/afterburning code[16] (LAPP) with and without the base region combustion products

* Note that this task was not directed at describing analytically all details of the complex flow regime in the base recirculation region.

as a boundary condition. This enables a direct comparison with the NO_x deposition rate due to afterburning computed in Ref. 2.

The composition of the base region combustion products was determined via a series of chemical equilibrium calculations for various ratios of the flow rates of freestream air and rocket exhaust products.* The equilibrium assumption is justified by the long residence times characteristic of the recirculation region. The plume calculations were made using the LAPP code[16] with the combustion products acting as a perturbation between the jet and the freestream.† The physical model for these calculations includes the following considerations: (1) the plume shock structure in the near field was determined via the AIPP code[14] and the universal plume shape correlation of Jarvinen and Hill[18] (see Fig. 14); (2) an equivalent single nozzle radius was assumed based on the geometry determined at the point of intersection of the two plumes;‡ (3) plume properties at this point were determined via single plume calculations using AIPP[14]; (4) the properties of the gas entrained from the base region were taken from that equilibrium calculation yielding the highest values of temperature and NO_x concentration. The initial conditions for the LAPP calculation are summarized in Table III.

B. Results

Some of the more important results of the base region equilibrium calculations are shown in Fig. 15, which plots the temperature and NO_x mole fraction vs. the molar ratio of exhaust to ambient air. Although the NO_x peak occurs at $X_{ex}/X_{air} = 0.5$, (X_{ex} = mole fraction of exhaust products), the peak temperatures occur at $X_{ex}/X_{air} > 2$. As a compromise, the base region gas composition and temperature were taken to be the values at $X_{ex}/X_{air} = 1.0$, where $[NO_x]$, [OH], [H] and temperature are all relatively high. The plume properties were calculated via LAPP[16] with the Smoot eddy viscosity correlations[19] and the chemistry scheme used in previous calculations.[2] The total

---

* The base pressure used for these calculations (which were made before we obtained the information from Park[10] on measured scale model shuttle base pressures) was 0.07 atm, taken from experimental results on a Saturn rocket at nearly the same altitude.[17] Use of ambient pressure at 30 km (0.0118 atm) for these calculations will not drastically alter the results.

† The mass flow of combustion products constituted 7% of the total plume mass flow. Because of the grid mesh requirements in LAPP, a smaller amount could not be used.

‡ The radius is $\sqrt{2}$ times the single plume radius at this point, or 30 ft.

TABLE III. INITIAL CONDITIONS FOR LAPP[16] CALCULATIONS

Effects of Base Region Combustion Products
on Plume [NO_x] Production;

Altitude = 30 km
Mach Number = 3.8

	Jet	Base	Freestream
Pressure, atm	0.01182	0.01182	0.01182
Temperature, °K	1200	2650	220
Velocity, fps	9800	5000	3750
Composition, mole fraction			
CO	2.31(-1)	8.92(-2)	
CO_2	2.24(-2)	5.11(-2)	
HCl	1.45(-1)	5.51(-2)	
H	4.17(-3)	3.32(-2)	
H_2	2.76(-1)	4.68(-2)	
OH	1.96(-4)	2.81(-2)	
H_2O	1.49(-1)	1.71(-1)	
N_2	9.45(-2)	4.52(-1)	0.79
N	2.78(-9)	1.00(-10)	
NO	1.85(-4)	6.74(-3)	
O	2.24(-5)	1.30(-2)	
O_2	5.33(-7)	1.97(-2)	0.21
Cl	3.85(-3)	2.72(-2)	
Al_2O_3	7.36(-2)	--	

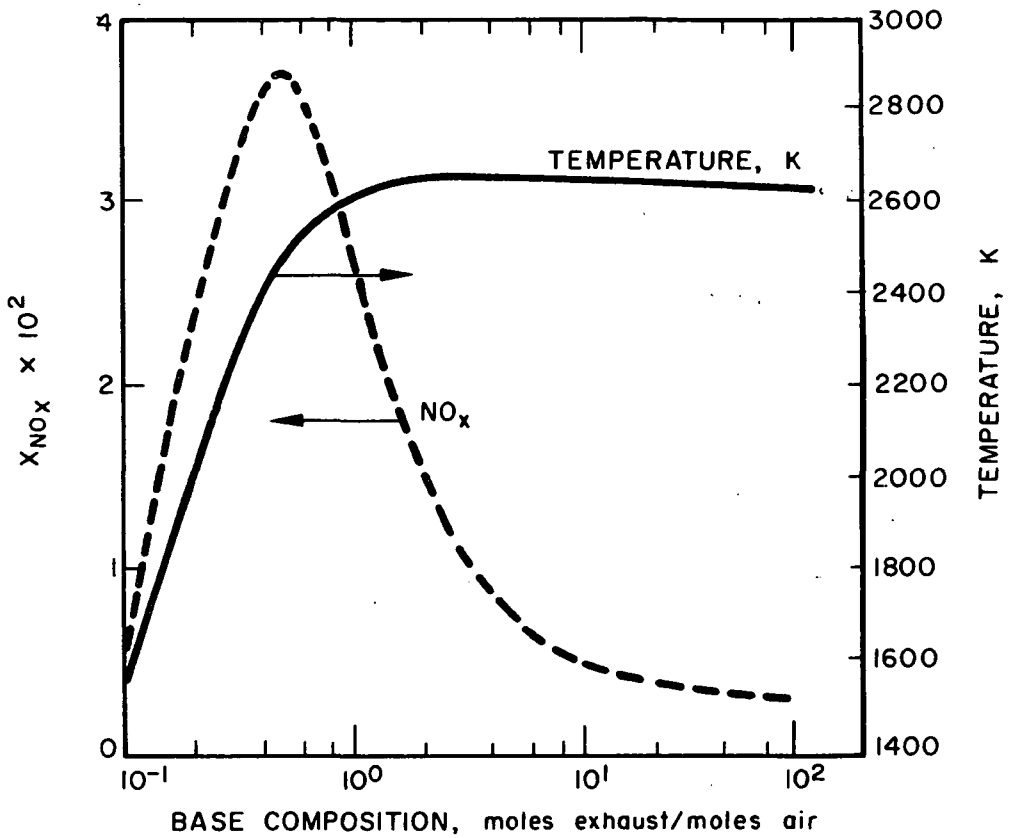

FIG. 15 EQUILIBRIUM TEMPERATURE AND NO_x MOLE FRACTION IN BASE RECIRCULATION REGION AS A FUNCTION OF COMPOSITION
P = 0.07 atm

mass flow of NO_x was determined by radial integration of local values from the axis to the edge of the plume. Calculations were made with and without the inclusion of the base region mass flux; the centerline temperature results are plotted in Fig. 16. Although these results indicate that more intense afterburning occurs due to entrainment of the base region combustion products, the effects of this afterburning on NO_x production were found to be neglibible. This is probably due to the relatively high level of NO_x, which is frozen near the nozzle throat (see Fig. 5), leaving the SRM.

The only significant increase in NO_x due to base region ignition effects would be that resulting from the NO_x found in the base region itself. Our base region equilibrium calculations show that $[NO_x]$ is about a factor of 35 greater than the exit plane value for $X_{ex}/X_{air} = 1.0$. Therefore, for example, if the mass entrained from the base region is 1% of the SRM mass flow rate, (probably a high value based on the considerations discussed in Section III) the maximum NO_x increase would be about 35%, well within the overall error limits of the entire analysis.

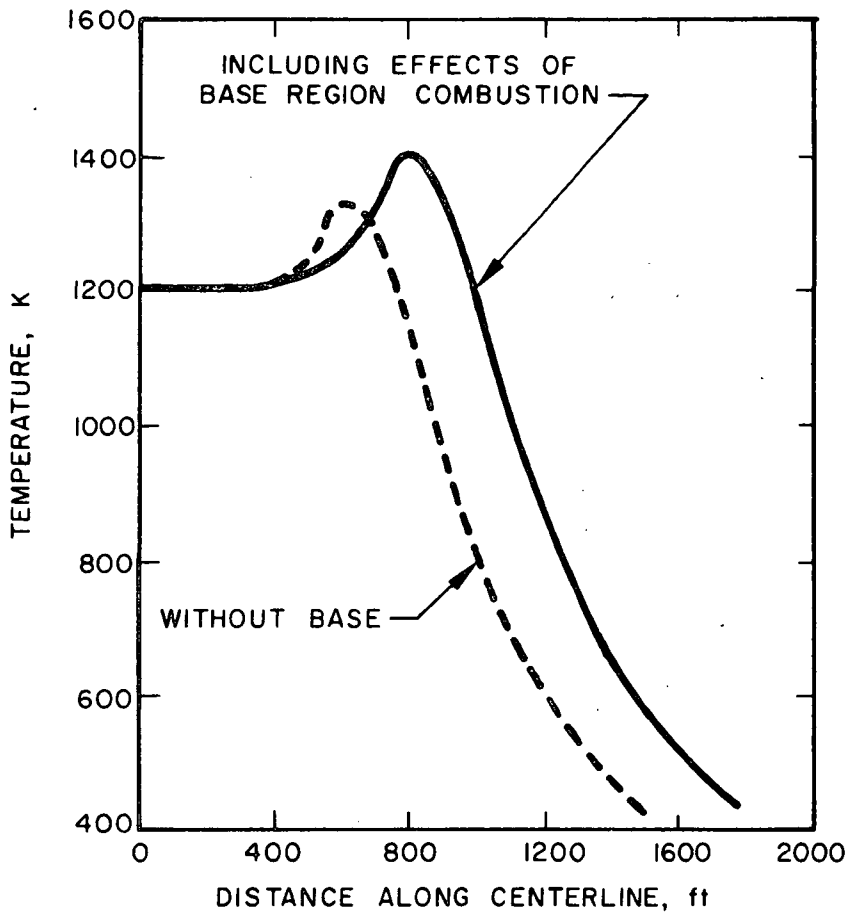

FIG. 16 EFFECTS OF BASE REGION COMBUSTION ON CENTERLINE TEMPERATURE

V. SUMMARY AND CONCLUSIONS

Under Phase I of this contract (see Ref. 2) the mass of NO_x deposited in the stratosphere by the space shuttle solid rocket motors was determined by assuming the twin SRM plumes could be replaced by an "equivalent" single nozzle plume having the same total mass flow. In this phase of the contract three separate effects were studied which could have potentially increased the NO_x deposition rate over that predicted from the equivalent single nozzle analysis: (1) uncertainties in Al_2O_3 particle sizes, size distributions and particle/gas drag and heat transfer coefficients, (2) intersection of the two SRM plumes and (3) combustion of SRM exhaust products in the shuttle base recirculation region. The results of the present study showed that none of these effects influence the initial prediction of plume NO_x deposition rate at 30 km altitude. It is therefore concluded that the NO_x mass flow "leaving" the plume at 30 km is 4000 g/sec with a possible error factor of $\overset{\times}{\div}$ 3. For a vehicle velocity of 1140 meter/sec this results in a NO_x deposition rate of about 3.5 g/meter. The corresponding HCl deposition rate at this altitude is about a factor of 500 greater than the NO_x deposition rate.

VI. REFERENCES

1. Whitten, R.C., Borucki, W.J., Poppoff, I.G. and Turco, R.P., "Preliminary Assessment of the Potential Impact of Solid-Fueled Rocket Engines in the Stratosphere," J. Atmos. Sci. 32, 613-619 (1975).

2. Pergament, H.S. and Thorpe, R.D., "NO_x Deposited in the Stratosphere by the Space Shuttle," AeroChem TN-161, Final Summary Report, NASA CR-132715, July 1975.

3. Pergament, H.S. and Mikatarian, R.R., "Prediction of Minuteman Exhaust Plume Electrical Properties," AeroChem TP-281, June 1973.

4. Pergament, H.S. and Thorpe, R.D., "A Computer Code for Fully-Coupled Rocket Nozzle Flows (FULLNOZ)," AeroChem TP-322, July 1975.

5. Smith, P.W., Delaney, L.J. and Radke, H.H., "Summary Results of Particle Size Measurements," in Proceedings of the AFRPL Two-Phase Flow Conference 1967, AFRPL-TR-67-223, Vol. I, p. 264.

6. Miller, R.R. and McCarty, K.P., "Metallic Fuel Agglomeration and Its Potential Role in Determining Rocket Motor Performance," ibid, p. 62.

7. Crowe, C.T., "On the Momentum and Heat Transfer Equations for Two-Phase Plumes," Washington State Univ., March 1971.

8. Penny, M., Lockheed Missiles and Space Co., Huntsville, AL, October 1975, private communication.

9. Roberts, B., NASA/JSC, May 1975, private communication.

10. Park, C., NASA/AMC, November 1975, private communication.

11. Goethert, B.H., "Studies of the Flow Characteristics and Performance of Multi-Nozzle Rocket Exhausts," AEDC-TR-59-16, October 1959.

12. Goethert, B.H. and Barnes, L.J., "Some Studies of the Flow Pattern at the Base of Missiles with Rocket Exhaust Jets," AEDC-TR-58-12, October 1958.

13. Pergament, H.S. and Kelly, J.T., "A Fully-Coupled Underexpanded Rocket Plume Program (The AIPP Code). Part 1. Analytical and Numerical Techniques," Final Report, AeroChem TP-302a, AFRPL-TR-74-59, NTIS AD/A 006 235, November 1974.

14. Pergament, H.S. and Kelly, J.T., "A Fully-Coupled Underexpanded Afterburning Rocket Plume Program (The AIPP Code). Part II. Program User's Manual," Final Report, AeroChem TP-328, AFRPL-TR-75-52, October 1975.

15. Draper, J.J., "The Role of the Plume Separated Region as a Flameholder on the Apollo Vehicle," AIAA Paper 75-243, 1975.

16. Mikatarian, R.R., Kau, C.J. and Pergament, H.S., "A Fast Computer Program for Nonequilibrium Rocket Plume Predictions," Final Report, AeroChem TP-282, AFRPL-TR-72-94, NTIS AD 751 984, August 1972.

17. Dixon, R.J. and Page, R.H., "Theoretical Analysis of Launch Vehicle Base Flow," Boeing Report No. D2-36605-1, June 1966.

18. Jarvinen, P.O. and Hill, J.A.F., "Universal Model for Underexpanded Rocket Plumes in Hypersonic Flow," CPIA Publ. No. 201, Vol. 1, 1975.

19. Stowell, D.E. and Smoot, L.D., "Turbulent Mixing Correlations in Free and Confined Jets," AIAA Paper 73-1194, 1973.